

Characterization of Single and Double Gate InSb Based HEMT Devices for High Frequency Application

R.Saravanakumar¹, A.Sarathi², C.Ramesh³Associate Professor, Department of Electronics and Communication Engineering, SKP Engineering College
Tiruvannamalai, Tamilnadu, India¹Assistant Professor, Department of Electronics and Communication Engineering, SKP Engineering College
Tiruvannamalai, Tamilnadu, India²Professor, Department of Electronics and Communication Engineering, SKP Engineering College Tiruvannamalai,
Tamilnadu, India³

ABSTRACT: We report the implementation of double gate symmetric Metal Oxide Semiconductor HEMT(DG-MOSHEMT) based on AlInSb/InSb material. The DG-MOSHEMT consist of 30nm gate length and it exhibit high transconductance (G_m), high cut off frequency (f_c) and maximum drain bias. We achieved greater $f_c=750$ GHz and $f_{max}=950$ GHz this result is higher than single gate AlInSb/InSb MOSHEMT. The High Electron Mobility Transistor (HEMT) is an important device for high speed, high frequency and microwave circuits.

KEYWORDS: IndiumAntimonide, MOSHEMT, symmetric MOSHEMT

I. INTRODUCTION

The Sb-based devices have intrinsic advantage of high speed and low power consumption that can provide the technology required for these application. In III-V narrow band gap semiconductors such as InAs and InSb have showed extremely high electron mobility because of their small electron effective mass [table1], which has brought about an increasing interest in themselves as promising channel materials for future logic, communication and terahertz devices.

The two-dimensional electron gas created at the interface between the channel and the barrier layers of High Electron Mobility Transistors (HEMT) provides a high concentration of electrons in the channel with very high mobility. In AlInSb/InSb particularly suitable for low-drain voltage operation, this material reduced DC-power consumption than GaAs. In Metal oxide Semiconductor HEMT(MOSHEMT) with insulating dielectrical are widely investigated, and excellent performance utilizing Al_2O_3 , TiO_2 , HfO_2 . In AlInSb/InSb MOSHEMT using Al_2O_3 as gate dielectric.

In symmetrical High electron mobility transistor the drain current(I_d) and transconductance (g_m) is high. In single gate High mobility electron transistor the short channel effect is high than compare to double gate. In double gate MOSHEMT in order to improve higher values of the transconductance over drain conduction ratio g_m/g_d and lower gate resistance R_g , these resulting improved the maximum oscillating frequency f_{max} .

International Journal of Innovative Research in Science, Engineering and Technology

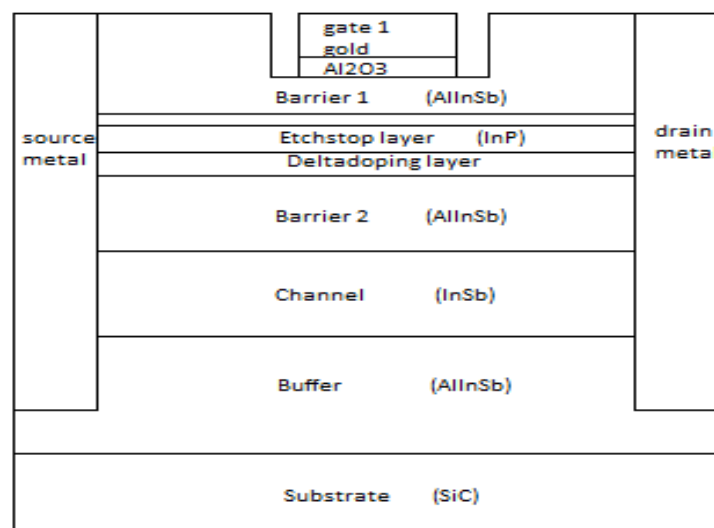
(An ISO 3297: 2007 Certified Organization)

Vol. 5, Issue 4, April 2016

	GaAs	InGaAs	InAs	InSb	units
Energy gap	1.43	0.75	0.356	0.175	eV
Electron effective mass	0.072	0.041	0.027	0.013	eV
Mobility for pure material	8500	14,000	30,000	78,000	cm ² V ⁻¹ s ⁻¹
Electron saturation velocity	1.2*10 ⁷	8*10 ⁸	3*10 ⁷	5*10 ⁷	cm s ⁻¹
Intrinsic carrier concentration	1.1*10 ⁷	5*10 ¹¹	1.3*10 ¹⁵	1.9*10 ¹⁶	cm ⁻³
Electron free mean path length	80	108	194	226	nm

Table[1] comparison of III-IV semiconductor materials

II. DEVICE STRUCTURE

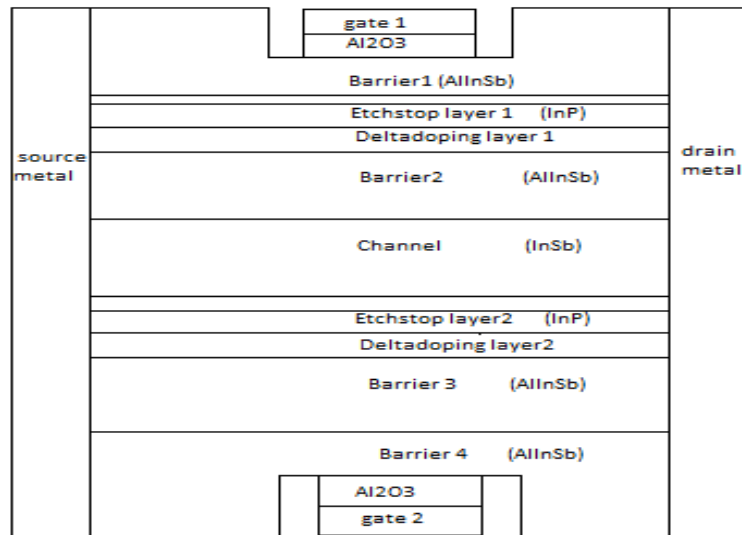


(a)

International Journal of Innovative Research in Science, Engineering and Technology

(An ISO 3297: 2007 Certified Organization)

Vol. 5, Issue 4, April 2016



(b)

Figure1:(a) & (b) Schematic diagram of single gate & double gate symmetric MOSHEMT based on AlInSb/InSb

In Figure1 shows the schematic illustration of the device geometry. In single gate symmetric MOSHEMT grown on 100nm SiC substrate. The barrier1/barrier2 are $\text{Al}_{0.15}\text{In}_{0.85}\text{Sb}$ with 14nm/15nm dimensions. The donor sheet density of the δ -doping layer is constant as $2.0 \times 10^{12} \text{ cm}^{-2}$. An etchstop layer placed above the δ -doping layer with 5nm for the purpose of controlling the threshold voltage. The source/drain are fabricated in metal with 50nm length and 70nm height. The distance of L_{sg} and L_{gd} are 5nm. The Oxide layer (Al_2O_3) placed below the gate with 3nm thickness. In double gate symmetric MOSHEMT barrier3/barrier4 are grown below the channel with 14nm/15nm dimensions.

III . RESULTS AND DISCUSSIONS

In Figure2, shows the V_g and I_d at source to gate voltage at 0.5V for single and double gate symmetric MOSHEMT. From this plot the double gate drain current (I_d) is higher than compare to single gate symmetric MOSHEMT. In Figure 3, shows the V_g and G_m for V_{gs} at 0.5V. In double gate symmetric MOSHEMT achieve greater transconductance (G_m) than compare to single gate MOSHEMT. The $\text{Al}_{0.15}\text{In}_{0.85}\text{Sb}$ Barrier/buffer, the electron distribution into the barrier as source to gate voltage increases, because of shallower quantum well (QW) channel.

In fig4, which shows the measurement of cut off frequency (f_T) versus gate voltage. At drain voltage 0.5V, anf_T of 500GHz for single gate MOSHEMT and 750 GHz for double gate symmetric MOSHEMT. From fig 5, shows the AlInSb/InSb device shows the maximum oscillation frequency (f_{max}) at drain voltage 0.5V. The estimated f_{max} in InSb devices at V_d 0.5V for single gate & double gate symmetric MOSHEMT are 550 GHz and 950 GHz respectively.

International Journal of Innovative Research in Science, Engineering and Technology

(An ISO 3297: 2007 Certified Organization)

Vol. 5 Issue 4 April 2016

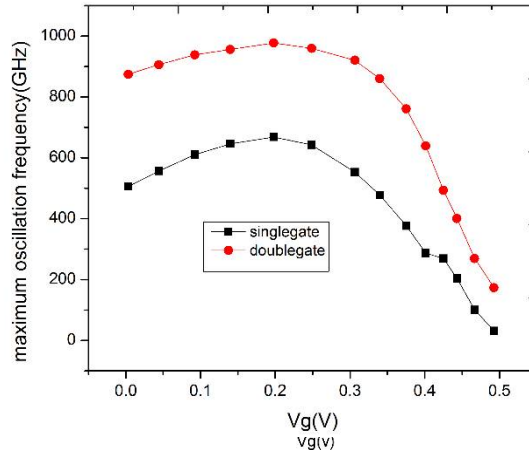


Figure 2, V_g and I_d as a function of V_{gs} at 0.5 V for single & double gate symmetric MOSHEMT .

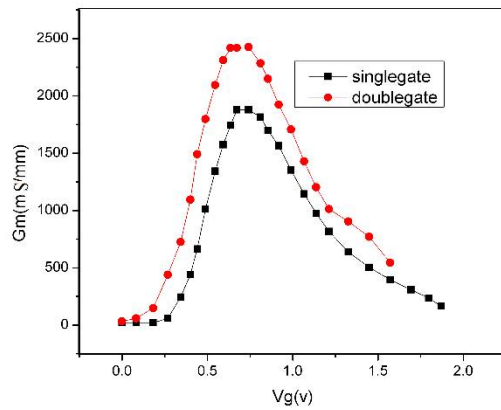


Figure 3, V_g and G_m function of V_{gs} at 0.5V for single & double gate symmetric MOSHEMT.

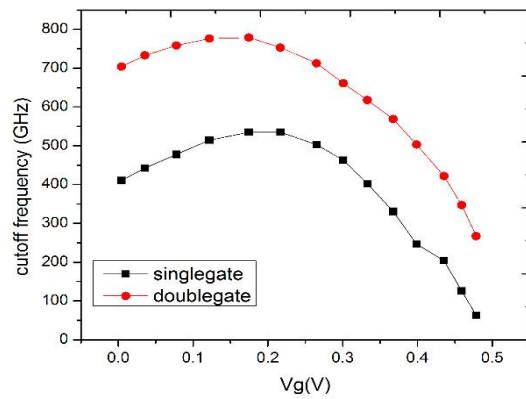


Figure4,cutoff frequency versus gate voltage of single & double MOSHEMT.

International Journal of Innovative Research in Science, Engineering and Technology

(An ISO 3297: 2007 Certified Organization)

Vol. 5, Issue 4, April 2016

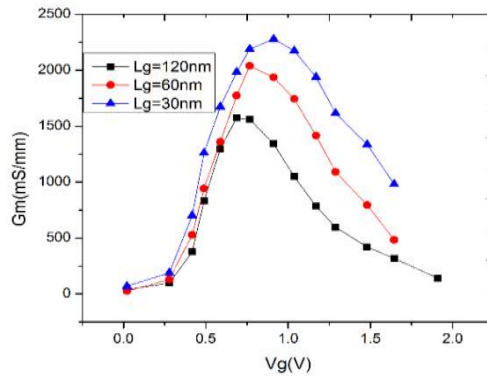


Figure5, maximum oscillation frequency versus gate voltage for single & double gate MOSHEMT.

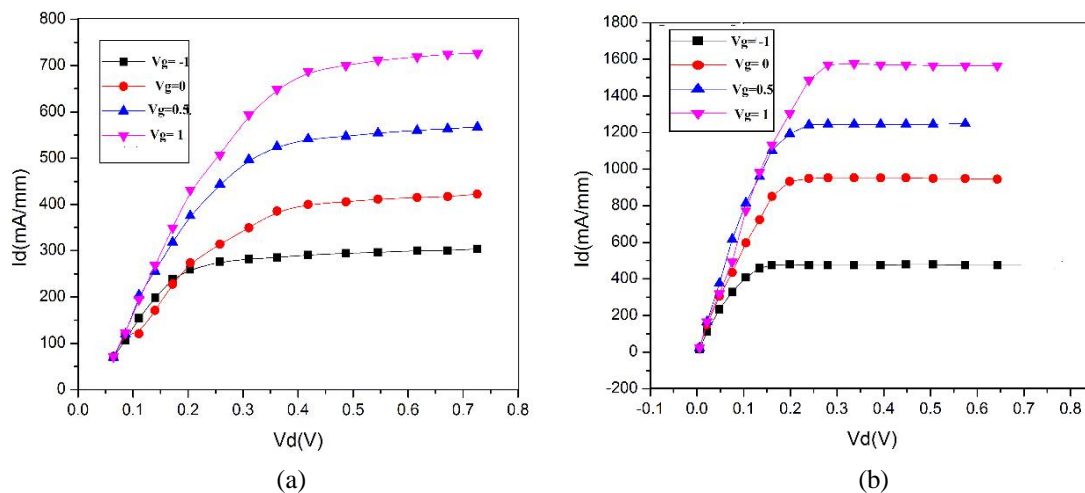


Figure6 : plot (a) and (b) shows the I_d versus V_{ds} characteristics of single & double gate MOSHEMT.

From fig 6, shows the InSb channel show I_d versus V_{ds} characteristics with L_g 30nm for single & double gate MOSHEMT at drain voltage 0.5 V. The gate voltage varies from -1.0 V to 1.0 V the corresponding drain current (I_d) increased in mA/mm. In this graph, the double gate MOSHEMT reaches the high drain current than single gate symmetric MOSHEMT. The device exhibits excellent pinch-off and drain current saturation behavior up to $V_d = 0.7$ V.

In fig 7, shows the V_g and G_m for different gate length at 0.5 V for single gate MOSHEMT. The different gate length the transconductance (G_m) increased. From the plot the different gate length are 120nm, 60nm and 30nm the corresponding transconductance values are increased 900, 1200 and 1400(mS/mm) respectively. In fig 8, shows different gate length at 0.5 V for double gate symmetric MOSHEMT. From the plot the different gate length are 120nm, 60nm and 30nm the corresponding transconductance values are increased 1500, 2000 and 2250 (mS/mm) respectively. Compare to double gate transconductance value is greater this make our device technology attractive for high – performance and very low power application.

International Journal of Innovative Research in Science, Engineering and Technology

(An ISO 3297: 2007 Certified Organization)

Vol. 5, Issue 4, April 2016

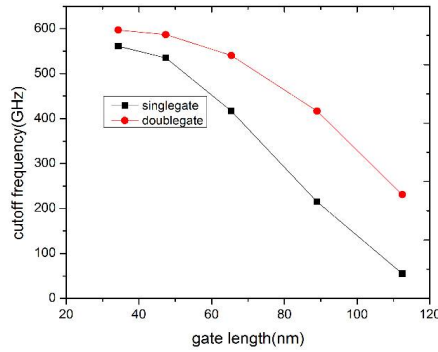


Figure 7, V_g versus G_m for different gate length at 0.5 V for single gate MOSHEMT.

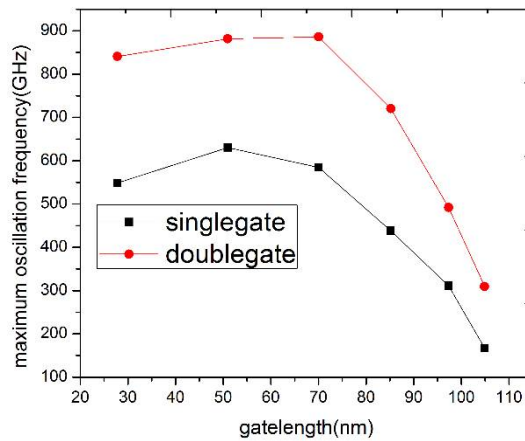


Figure 8, V_g and G_m for different gate length double gate MOSHEMT.

From fig 9, shows cutoff frequencies (f_T) versus different gate length in nm at drain voltage at 0.5V. In different gate length the cutoff frequencies are increased. From the plot the different gate length are 120nm, 90nm, 70nm, and 30nm the corresponding cutoff frequencies are 100GHz, 200GHz, 400GHz and 550GHz respectively. From the relation $f_T = G_m / C_{ox}$ the transconductance (G_m) increased it leads to high cutoff frequencies.

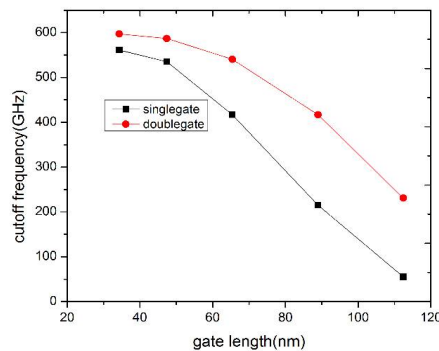


Figure 9, cutoff frequencies versus different gate length in nm at drain voltage 0.5V for single & double gate MOSHEMT.

International Journal of Innovative Research in Science, Engineering and Technology

(An ISO 3297: 2007 Certified Organization)

Vol. 5, Issue 4, April 2016

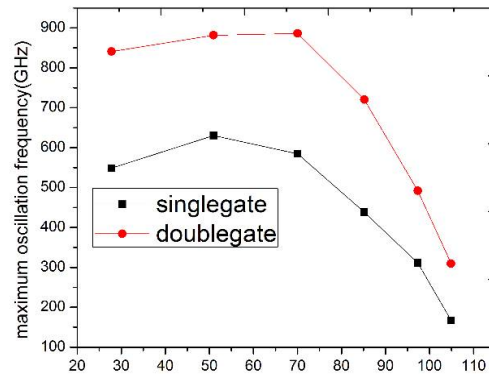


Figure 10, maximum oscillation frequency versus gatlength in nm at drain voltage 0.5V for single and double gate MOSHEMT.

In fig10, the f_{max} versus V_g at drain voltage 0.5 V for single and double gate symmetric MOSHEMT. In single gate the different gate length are 30nm, 70nm, 100nm and 110nm the corresponding f_{max} are 550GHz, 500GHz, 350GHz, 100GHz respectively. In double gate MOSHEMT the gatlength are reduced the frequencies are increased. The different gate length are 110nm, 100nm, 70nm, 30nm the corresponding frequencies values are 300GHz, 550GHz, 800GHz, 850GHz respectively.

IV. CONCLUSION

We have demonstrated InSb quantum well transistors down to 30nm gatlength with comparable high frequency performance to today's Si MOSFET's. The device exhibit excellent transfer and output characteristics to extract current voltage curves. Frequency analysis predicted a cutoff frequency $f_T = 750$ GHz and a maximum oscillation frequency $f_{max} = 950$ GHz for double gate symmetric MOSHEMT. In future work, according to Moore's law requires continuous scaling of Si MOSFETs. The physical gatlength of Si – transistors that are utilized is about 100nm. It is expected that critical dimension will reach about 10nm in the future to improve the transfer, output and RF characteristics of these devices to improve the high performance with low power.

REFERENCES

- [1] S. Datta *et al.*, "85nm Gate Length Enhancement and Depletion mode InSb Quantum Well Transistors for Ultra High Speed and Very Low Power Digital Logic Applications," *2005 IEEE IEDM Tech. Dig.*, pp. 763-766, 2005.
- [2] Dae-Hyun Kim *et al.*, " $f_T = 688$ GHz and $f_{max} = 800$ GHz in $L_g = 40$ nm In_{0.7}Ga_{0.3}As MHEMTs with $gm_{max} > 2.7$ mS/ μ m," *2011 IEEE IEDM. Tech. Dig.*, pp. 13.6.1-13.6.4, 2011.
- [3] H. Nishino *et al.*, "Monte Carlo Study of Strain Effect on High Field Electron Transport in InAs and InSb," *2010 IPRM Proceedings*, pp. 156-159, 2010.
- [4] F. Machida *et al.*, "Strain Effects on Performances in InAs HEMTs," *2011 IPRM Proceedings*, pp. 437-440, 2011.
- [5] S. Hara *et al.*, "Quantum-Corrected Monte Carlo Simulation of InSb HEMTs Considering Strain Effects," *2011 TWHM Abstracts*, p. 41, 2011.
- [6] H. I. Fujishiro *et al.*, "Quantum Corrected Monte Carlo Analysis of Scaling Behavior of Nano-Scale InGaAs High Electron Mobility Transistors," *2007 ISCS Abstracts*, pp. 2795- 2798, 2007.
- [7] D.-H.Kim and J.A.del Alamo, *IEEE Electron Device Lett.*, Vol.29, pp.830-833, 2008.
- [8] T.Takegishi, H.Watanabe, R.Yamada, T.Matsumoto, S.Hara and H.I.Fujishiro, in *Proc. IPRM*, pp.124-127, 2009.
- [9] Y.Hori, Y.Ando, Y.Miyamoto, and O.Sugino, *Solid State Electronics*, vol.43, pp.1813-1816, 1999.
- [10] T.Mizuno, S.Takagi, N.Sugiyama, H.Satake, A.Kurobe, and A.Toriumi, *IEEE Electron Device Lett.*, Vol.21, pp.230-232, 2000.
- [11] K.Brennan and K.Hess, *Solid State Electronics*, vol.27, pp.347-357, 1984.
- [12] D.C.Herbert, P.A.Children, Richard A.Abram, G.C.Crow, and M.Walmsley, *IEEE Trans. on Electron Devices*, vol. 52, pp.1072-1078, 2005.
- [13] H.Rodilla, T.Gonzalez, D.Pardo, and J.Mateos, *J.Appl. Phys.*, vol. 105, pp.1-6, 2009.
- [14] V.Chandramouli and C.M.Maziar, *Solid State Electronics*, vol.36, pp.285-290, 1993.
- [15] S.C.Jain, J.R.Willis, and R.Bullough, *Adv. Phys.* 39, pp.127-190, 1990.
- [16] M.L.Cohen and T.K.Bergstresser, *Phys. Rev.*, vol.141, pp. 789-796, 1966.
- [17] M.M.Rieger and P.Vogl, *Phys. Rev. B*, vol. 48, pp. 14276-14287, 1993.
- [18] J.A.Sanjurjo, E.Lopez-Cruz, P.Vogl, and M.Cardona, *Phys. Rev. B*, vol.28, pp.4579-4584, 1983.
- [19] C.L.Anderson and C.R.Crowell, *Phys. Rev. B*, vol. 15, pp.2267-2272, 1972.